High-repetition-rate quasi-CW side-pumped mJ eye-safe laser with a monolithic KTP crystal for intracavity optical parametric oscillator

C. Y. Cho,[1] Y. C. Chen,[1] Y. P. Huang,[2] Y. J. Huang,[1] K. W. Su,[1] and Y. F. Chen[1,*]

[1]*Department of Electrophysics, National Chiao Tung University, Hsinchu, Taiwan*
[2]*Department of Physics, Soochow University, Shih Lin, Taipei, Taiwan*
[*]*yfchen@cc.nctu.edu.tw*

Abstract: We demonstrate a high-repetition-rate millijoule passively Q-switched eye-safe Nd:YVO_4 laser pumped by a quasi-CW diode stack. A theoretical analysis has been explored for the design criteria of generating $TEM_{n,0}$ mode in the diode-stack directly side-pumping configuration. We successfully generate $TEM_{n,0}$ modes at 1064 nm by adjusting the gain medium with respected to the laser axis. We further observe the spatial cleaning ability for generating an nearly $TEM_{0,0}$ mode output at 1573 nm with a monolithic OPO cavity. At the repetition rate up to 200 Hz, the output pulse energy reaches 1.21 mJ with the threshold pump energy of 17.9 mJ.

OCIS codes: (140.3480) Lasers, diode-pumped; (140.3540) Lasers, Q-switched; (140.3530) Lasers, neodymium.

References and links

1. E. Gregor, D. E. Nieuwsma, and R. D. Stultz, "20 Hz eyesafe laser rangefinder for air defense," Proc. SPIE **1207**, 124–135 (1990).
2. W. Krichbaumer, H. Herrmann, E. Nagel, R. Haring, J. Streicher, C. Werner, A. Mehnert, T. Halldorsson, S. Heinemann, P. Peuser, and N. P. Schmitt, "A diode-pumped Nd:YAG lidar for airborne cloud measurements," Opt. Laser Technol. **25**(5), 283–287 (1993).
3. J. E. Nettleton, B. W. Schilling, D. N. Barr, and J. S. Lei, "Monoblock laser for a low-cost, eyesafe, microlaser range finder," Appl. Opt. **39**(15), 2428–2432 (2000).
4. W. Zendzian, J. K. Jabczynski, P. Wachulak, and J. Kwiatkowski, "High-repetition-rate, intracavity-pumped KTP OPO at 1572 nm," Appl. Phys. B **80**(3), 329–332 (2005).
5. L. R. Marshall and A. Kaz, "Eye-safe output from noncritically phase-matched parametric oscillators," J. Opt. Soc. Am. B **10**(9), 1730–1736 (1993).
6. B. W. Schilling, S. R. Chinn, A. D. Hays, L. Goldberg, and C. W. Trussell, "End-pumped 1.5 microm monoblock laser for broad temperature operation," Appl. Opt. **45**(25), 6607–6615 (2006).
7. F. F. Wu and J. W. Pierce, "An eye-safe optical parametric oscillator system with more than 5 megawatts peak power," Proc. SPIE **7686**, 768609 (2010).
8. W. Koechner, *Solid-State Laser Engineering,* 6th ed. (Springer, 2006).
9. R. Beach, J. Davin, S. Mitchell, W. Benett, B. Freitas, R. Solarz, and P. Avizonis, "Passively Q-switched transverse-diode-pumped Nd^{3+}:YLF laser oscillator," Opt. Lett. **17**(2), 124–126 (1992).
10. Y. F. Chen, S. W. Chen, Y. C. Chen, Y. P. Lan, and S. W. Tsai, "Compact efficient intracavity optical parametric oscillator with a passively Q-switched Nd:YVO_4/Cr^{4+}:YAG laser in a hemispherical cavity," Appl. Phys. B **77**(5), 493–495 (2003).
11. Y. F. Chen, S. W. Tsai, and S. C. Wang, "High-power diode-pumped Q-switched and mode-locked Nd:YVO_4 laser with a Cr^{4+}:YAG saturable absorber," Opt. Lett. **25**(19), 1442–1444 (2000).
12. Y. F. Chen, Y. P. Lan, and H. L. Chang, "Analytical model for design criteria of passively Q-switched lasers," IEEE J. Quantum Electron. **37**(3), 462–468 (2001).
13. J. Y. Huang, W. Z. Zhuang, Y. P. Huang, Y. J. Huang, K. W. Su, and Y. F. Chen, "Improvement of stability and efficiency in diode-pumped passively Q-switched intracavity optical parametric oscillator with a monolithic cavity," Laser Phys. Lett. **9**(7), 485–490 (2012).
14. A. Cotel, A. Jullien, N. Forget, O. Albert, G. Cheriaux, and C. Le Blanc, "Nonlinear temporal pulse cleaning of a 1-μm optical parametric chirped-pulse amplification system," Appl. Phys. B **83**(1), 7–10 (2006).
15. K. Kubodera and K. Otsuka, "Single-transverse-mode $LiNdP_4O_{12}$ slab waveguide laser," J. Appl. Phys. **50**(2), 653–659 (1979).
16. Y. F. Chen, T. M. Huang, C. F. Kao, C. L. Wang, and S. C. Wang, "Generation of Hermite-Gaussian modes in fiber-coupled laser-diode end-pumped lasers," IEEE J. Quantum Electron. **33**(6), 1025–1031 (1997).

#205652 - $15.00 USD Received 28 Jan 2014; revised 25 Feb 2014; accepted 26 Feb 2014; published 25 Mar 2014

17. M. D. Wei, C. C. Cheng, and S. S. Wu, "Instability and satellite pulse of passively Q-switching Nd:$LuVO_4$ laser with Cr^{4+}:YAG saturable absorber," Opt. Commun. **281**(13), 3527–3531 (2008).

1. Introduction

Millijoule (mJ) eye-safe lasers have plenty applications in remote sensing, range finder or airborne lidar, etc [1–3]. In addition, mJ laser pulses with repetition rate up to hundreds of Hz can be utilized in specific regions like lidar system required high-speed data collection. Diode-pumped solid-state laser with the emission wavelength at near-infrared region plays an important role for obtaining eye-safe laser through the process of optical parametric oscillator (OPO) [4,5]. Recently, quasi-CW (QCW) diode stacks have been widely used in high-pulse-energy lasers as pump sources due to high power intensities [6,7]. However, the maximum duty for conventional QCW diode stacks usually must be 2-4%. This limitation leads to the available pump duration to be in the range of 100 to 200 μs for a repetition rate higher than 200 Hz. Therefore, although Nd:YAG and Nd:YLF crystals are often used in high-pulse-energy laser systems [8], the Nd:YVO_4 crystal with a relatively short upper level lifetime can be employed to obtain higher efficiencies in QCW diode-stack pumped lasers with a repetition rate higher than 200 Hz. Furthermore, compared to other Nd-doped crystals, the Nd:YVO_4 crystal has a wider absorption bandwidth at the optimum pump wavelength. This advantage enables the diode-pumped Nd:YVO_4 lasers to be operated in a wider temperature range. More importantly, the *a*-cut Nd:YVO_4 crystal can directly provide a linearly polarized output beam that is particularly useful for the process of nonlinear wavelength conversions. Therefore, it is highly desirable to explore the QCW diode-stack pumped Nd:YVO_4 laser with a repetition rate up to 200 Hz and an output energy higher than mJ.

To achieve high conversion efficiency for OPO, using passively Q-switched (PQS) near-infrared laser with high peak power is a great method thanks to the low-cost and easily controlled feature [8]. Utilizing QCW diode stack with a large pump area to side pump a PQS laser can contribute to higher output pulse energies since the laser mode size is proportional to the output pulse energy of the PQS laser. Nevertheless, the output transverse mode tends to be multimode with the degradation of the beam quality [9]. In this work, we demonstrated a fundamental-mode Nd:YVO_4/KTP/Cr^{4+}:YAG eye-safe laser side-pumped by a QCW diode stack. A theoretical analysis have been explored for the design criteria of generating $TEM_{n,0}$ mode in the directly diode-stack side-pumping configuration by adjusting the active medium with respect to the laser axis. The laser resonator was a hemispherical cavity applied to reach the second threshold condition of the PQS laser [10–12]. Furthermore, the cavity mode size on the gain medium can be significantly enlarged for mode matching. We confirmed the threshold dependence with the theoretical model at 1064 nm and successfully generated a $TEM_{0,0}$ mode output. For the 1573-nm laser, a monolithic intracavity OPO (IOPO) cavity was used to separate the infrared and eye-safe resonators for optimization [13]. We further observed the spatial cleaning ability for the OPO resonator. With nearly $TEM_{0,0}$-mode output, the output pulse energy was 1.21 mJ at 17.9 mJ pump energy and the repetition rate up to 200 Hz [14].

2. Theoretical analysis and experimental setup

The experimental setup for the eye-safe laser is shown in Fig. 1. The gain medium is a 0.5 at. % *a*-cut Nd:YVO_4 crystal with dimension of $3 \times 3 \times 12$ mm^3. Both end surface were coated for anti-reflection (AR, R<0.2%) at 1064 nm. We cut two end surfaces with 2-degree wedge to prevent the parasitic pulse. The pump surface was AR coated at 808 nm. We utilized a 2-mm long Cr^{4+}:YAG with an initial transmittance of 35% as a PQS saturated absorber. A non-critical phase-matching (*x*-cut) KTP crystal with dimension of $3 \times 3 \times 20$ mm^3 was applied as an IOPO nonlinear crystal. Notice that the OPO resonator was coated on the surfaces of the KTP crystal to separate the 1064-nm and 1573-nm cavity for optimization. The first end facet was coated for high-transmission (HT, T>95%) at 1064 nm and high-reflection (HR, R>99.8%) at 1573 nm. The second end facet was coated for HT at 1064 nm and partial reflection (R = 50%) at 1573 nm. All three crystals were wrapped with indium foil and

#205652 - $15.00 USD Received 28 Jan 2014; revised 25 Feb 2014; accepted 26 Feb 2014; published 25 Mar 2014

mounted in conductively water-cooled copper blocks. The pump source was a four-bar high-power diode stack (Coherent G-stack package, Santa Clara, Calif., USA) with emission wavelength at 808 nm. Each bar was 10 mm long and the pitch between them was 0.4 mm, which consist approximately 10 × 1.2-mm^2 pumping area. The diode stack emitting side was placed with a distance d against the side facet of the Nd:YVO_4 crystal directly for compact design. We mounted the diode stack with the Nd:YVO_4 crystal and adjusted them simultaneously on the horizontal axis with respect to the laser axis to explore generation of $TEM_{n,0}$ mode at 1064 nm.

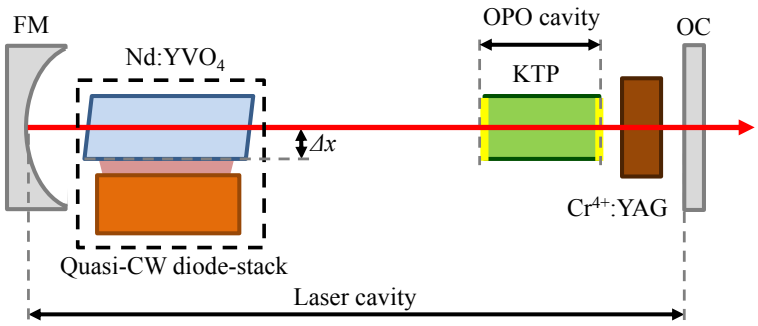

Fig. 1. Experimental setup for the Nd:YVO_4 laser.

The threshold power for $TEM_{n,0}$ mode is given by calculating the overlapping of the pumping and emission area [15,16]

$$P_{th}(TEM_{n,0}) = \frac{\gamma I_{sat}}{\eta_p L} \frac{1}{\iiint s_{n,0}(x,y,z) r_p(x,y,z) dv}, \tag{1}$$

where γ is the total cavity loss per pass, I_{sat} is the saturation intensity, η_p is the efficiency constant related to the energy levels of the laser crystal, L is the length of the gain medium. $s_{n,0}(x,y,z)$ is the normalized cavity mode intensity distribution and $r_p(x,y,z)$ is the normalized pump intensity distribution in the active medium. Considering a displacement, Δx , for the active medium with respect to the laser axis, the single transverse mode distribution can be given by

$$s_{n,0}(x-\Delta x, y) = \frac{2}{\pi \omega_0^2 2^n n!} H_n^2\left(\frac{\sqrt{2}(x-\Delta x)}{\omega_0}\right) \exp\left(\frac{-2[(x-\Delta x)^2 + y^2]}{\omega_0^2}\right), \tag{2}$$

where $H_n()$ is the Hermite polynomial of order n, ω_0 is the cavity mode size in the gain medium, which is approximated to be constant along the laser axis. The diode-stack pump intensity distribution in the gain medium can be given by the sum of each diode bar

$$r_p(x,y) = \sum_{m=0}^{M-1} R_p\left\{x, y - \left[mD - \left(\frac{M-1}{2}\right)D\right]\right\}, \tag{3}$$

where M is the total number of the diode bar, D is the pitch between each diode bar, $R_p(x, y-\xi)$ is the pump distribution of each diode bar at different height, ξ. We assumed that the pump distribution on laser axis was uniform. Then $R_p(x, y-\xi)$ is given by

$$R_p(x, y-\xi) = \frac{\sqrt{2}\alpha}{\sqrt{\pi}\omega_y(x)} \exp\left(-\alpha\sqrt{x^2 + (y-\xi)^2}\right) \exp\left(-\frac{2(y-\xi)^2}{\omega_y^2(x)}\right), \tag{4}$$

#205652 - $15.00 USD Received 28 Jan 2014; revised 25 Feb 2014; accepted 26 Feb 2014; published 25 Mar 2014

where α is the absorption coefficient of the gain medium at the pump wavelength. $\omega_y(x)$ is the diode-bar mode size changed along fast axis, which is given by

$$\omega_y(x) = \omega_{y0}\sqrt{1+\left[\frac{M_y\lambda_p(x-d)}{\pi\omega_{y0}^2 n}\right]^2}, \tag{5}$$

where ω_{y0} is the beam waist on the diode bar, M_y is the fast-axis beam quality factor of the diode bar, λ_p is the pump wavelength, n in the reflected index of the pump wavelength. Notice that d is the distance between the diode bar and the pump surface of the active medium. Using Eqs. (2)–(5), we can depict the pump and mode distribution on the active medium with the transverse dimension of 3 × 3 mm^2 as showed in Fig. 2. For our experiment, the diode-stack was placed with a fixed distance against the active medium d = 2 mm. From, Fig. 2(a), we can easily observe the asymmetry of the side-pumping configuration. The mode distribution for $TEM_{0,0}$ mode was calculated with Δx = 1 mm for overlapping the pump distribution. From Fig. 2(d), we can observe that the pattern of the $TEM_{2,0}$ mode was cut by the edge of the active medium since the cavity mode size for the side-pumping scheme is usually designed to be much larger than that of the end-pumping scheme. In our analysis, we utilized the cavity mode size of ω_0 = 0.85 mm to match the pumping area. The other calculating parameters are as follow: α = 0.55 mm^{-1}, ω_{y0} = 0.834 mm, M_y = 1.0, and n = 2.16.

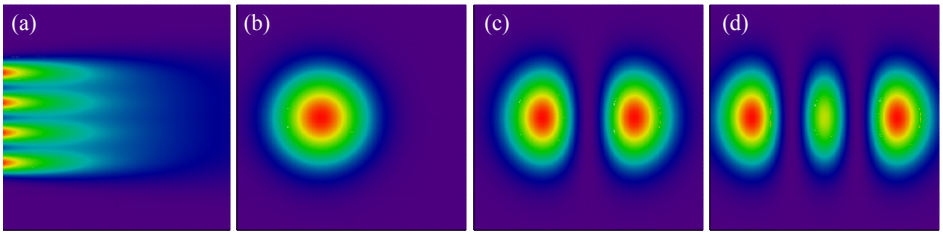

Fig. 2. Calculated transverse intensity distribution on the gain medium for (a) pump source, (b) $TEM_{0,0}$ mode, (c)$TEM_{1,0}$ mode and (d) $TEM_{2,0}$ mode.

Considering the large cavity mode size, we apply the loss factor, γ, to be inversely proportional to the area of the mode distributed in the crystal. We denote $\gamma_{n,0}(\Delta x)$ as the loss factor which is related to the order of the transverse mode and the displacement of the active medium. Noticed that we assume the distributions on the laser axis are uniform for both pumping and emitting area. With the same pump source and gain medium, we can further obtain that the threshold multiplied a constant N was inversely proportional to the overlapping of the pumping and emitting area, which can be given by

$$NP_{th}(TEM_{n,0}) = \gamma_{n,0}(\Delta x)\left[\int_{-b}^{b}\int_{0}^{2a} s_{n,0}(x-\Delta x, y)r_p(x,y)dxdy\right]^{-1}, \tag{6}$$

where a is half of the width and b is half of the height for the active medium. With Eqs. (2)–(6), we can obtain the relation of the threshold tendency, $NP_{th}(TEM_{n,0})$, with respect to the displacement Δx. From Fig. 3, we can observe that the $TEM_{0,0}$ mode can be generated by moving the active medium with approximately 0.8 mm. On the other hand, the threshold for $TEM_{2,0}$ mode is always larger than $TEM_{1,0}$ mode.

For the laser resonator, we applied a 250-mm-radii-of-curvature concave mirror as the front mirror with HR coated at 1064 nm. The resonator was a nearly hemispherical cavity to

#205652 - $15.00 USD Received 28 Jan 2014; revised 25 Feb 2014; accepted 26 Feb 2014; published 25 Mar 2014

reach the second threshold condition of the passive Q-switching and for the mode-matching. For the fundamental laser at 1064 nm, we applied a plane output coupler with first and second facets coated to be partial reflection (R = 60%) and AR, respectively, at 1064 nm. For the IOPO laser at 1573 nm, we utilized a plane output coupler with the first surface coated to be HR at 1064 nm and HT at 1573 nm and the second surface coated to be AR at both 1064 and 1573 nm. We used a LeCroy digital oscilloscope (Wavepro 7100, 10 G samples/s, 1 GHz bandwidth) with a fast InGaAs photodiode to record the pulse temporal behaviors. The laser beam profiles were recorded by a HAMAMATSU CCD camera (INFRARED VIDCON CAMERA, C2741-03) and the emission wavelength was recorded by an ADVANTEST optical spectrum analyzer with resolution of 0.1 nm (Q89381A).

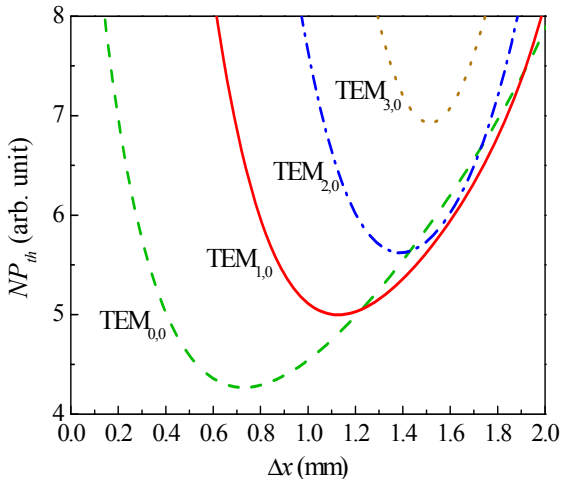

Fig. 3. Calculated results of the threshold tendency with respect to the displacement of the gain medium for generating $TEM_{n,0}$ mode.

3. Experimental results

In the first place, we demonstrated the free-running operation without Cr^{4+}:YAG and KTP crystals to confirm the reliability of the laser resonator. The pumping pulse width was set to be 100 μs to match the upper level lifetime of the Nd:YVO_4 crystal. By continuously moving the active medium from Δx = 0 mm, we observed that the $TEM_{0,0}$ mode was generated at approximately Δx = 0.3 mm and the transverse pattern changed into $TEM_{1,0}$ mode at approximately Δx = 1.2 mm. With Δx larger than 1.5 mm, the laser was unable to emit. We further confirmed that the $TEM_{2,0}$ mode was not realized since the threshold energy was relatively high. The observed threshold tendency was quite coincided to the theoretical analysis as shown in Fig. 3. Then we compared the output pulse energy for each mode. The largest output energy for $TEM_{0,0}$ mode and $TEM_{1,0}$ mode appeared at Δx = 0.9 mm and 1.3 mm, respectively. Figure 4 shows the output pulse energy at 1064 nm with respect to the incident pump energy at 808 nm. The slope efficiency and the threshold energy for $TEM_{0,0}$ mode were approximately 43.8% and 2.9 mJ, respectively. For $TEM_{1,0}$ mode, the threshold energy increased to approximately 3.4 mJ with the slope efficiency up to 52.3%.The transverse mode distributions were also showed in Fig. 4.

#205652 - $15.00 USD Received 28 Jan 2014; revised 25 Feb 2014; accepted 26 Feb 2014; published 25 Mar 2014

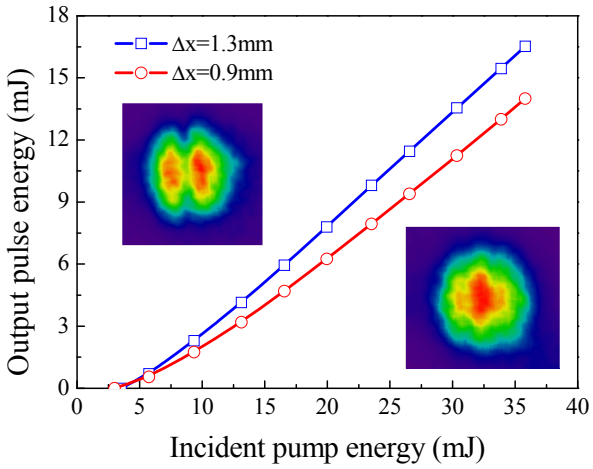

Fig. 4. Output energies at 1064 nm under free-running operation with respect to the incident pump energy of laser diode-stack. The inset: transverse mode distributions for $TEM_{0,0}$ mode and $TEM_{1,0}$ mode.

For the PQS laser, we placed the saturated absorber 25 mm from the output coupler to prevent the damage on the crystal. The largest output pulse energy was found to be 3.05 mJ at the threshold pump energy of 19.6 mJ. It can be anticipated that a Cr^{4+}:YAG crystal with lower transmittance was able to enlarge the output pulse energy with larger input pump energy. However, the saturated absorber would be easily damaged because of the extremely high intensity on the saturated absorber. It was worth to mention that the transverse distribution with the maximum output pulse energy was also observed as $TEM_{1,0}$ mode at Δx = 1.3 mm. Furthermore, the output pattern at Δx = 0.9 mm was observed to be nearly $TEM_{0,0}$ mode with the output pulse energy and the threshold energy decreased to 2.81 mJ and 18.2 mJ, respectively. We also confirmed that the $TEM_{2,0}$ mode was not able to be generate. The threshold dependence of the $TEM_{n,0}$ mode on the displacement Δx for the PQS operation were completely corresponded to the results found with free-running operation, which were all consistent with the theoretical analysis. The highest repetition rate for the PQS laser was observed to be 200 Hz. Repetition rate higher than this region would lead to the decrease of the output pulse energy. We believed that it was due to the serious thermal lensing effect on the laser crystal, which would make the cavity step into the unstable region. Shortening the cavity length might solve this problem; however, the mode size on both gain medium and saturated absorber would be smaller, and the pump-to-mode-size and the second threshold condition would be mismatched. Furthermore, this approached would easily cause damage on the Cr^{4+}:YAG crystal. Figure 5 shows the temporal pulse shapes for the PQS laser. The pulse width was approximately 13 ns and the calculated peak power was 0.11 MW. We found out that for Δx = 1.3 mm, the output laser pulse would sometimes appear with a satellite pulse. The probabilities of generating a pulse with and without the satellite pulse were nearly the same. On the other hand, the pulse shape was unlikely to have the satellite pulse for Δx = 0.9 mm, which showed that the fundamental mode was more likely to produce a pure pulse [17].

For the eye-safe laser, we inserted a monolithic KTP crystal coated with the OPO cavity on both facets and changed the output coupler. We observed that the output pulse energy at 1573 nm was approximately 1.21 mJ with the threshold energy of 17.9 mJ and the repetition rate of 200 Hz. The optical spectrum and the temporal shape for the IOPO pulse are showed in Figs. 6(a) and 6(b), respectively. The temporal pulse shapes were recorded by utilizing a plane mirror coated to be HT at 1064 nm and HR 1573 nm to separate the emission wavelength. The pulse width of the first peak for the signal pulse at 1573 nm was approximately 2.3 ns and the calculated peak power was 61 kW. Figure 6(b) also shows that the 1064-nm pulse was eliminated by the 1573-nm pulse. It was worth to mention that the

#205652 - $15.00 USD Received 28 Jan 2014; revised 25 Feb 2014; accepted 26 Feb 2014; published 25 Mar 2014

depleted pulse energy at 1064 nm was observed to be smaller than 0.01 mJ since the output coupler was coated with HR coating at 1064 nm. We further observed that the satellite pulse was disappeared when the KTP crystal was inserted and the pattern for the IOPO laser was observed to be nearly TEM_{00} mode, which is shown in Fig. 6(c). The beam quality factor for the 1573 nm was measured to be approximately 1.4 × 1.5 (vertical × horizontal). We also confirm that the transverse mode did not depend on the displacement of the gain medium, Δx . The results of the pattern changed between PQS and IOPO configuration can be explained by the ability of spatial cleaning for the OPO resonator.

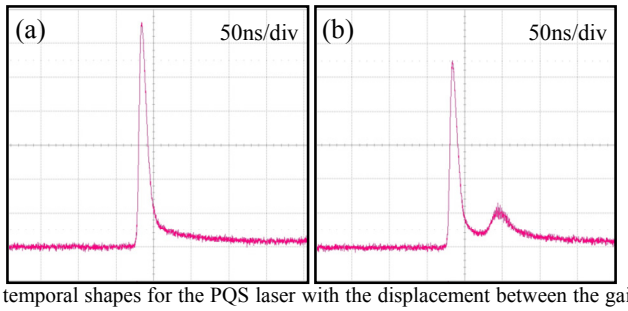

Fig. 5. The temporal shapes for the PQS laser with the displacement between the gain medium and the laser diode-stack, Δx , equal to (a) 0.9 mm and (b) 1.3 mm.

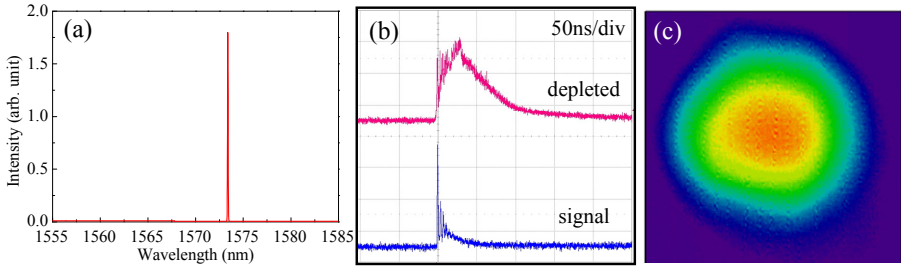

Fig. 6. The output performance for the IOPO laser: (a) The emission wavelength, (b) the temporal shapes, and (c) the transverse distribution.

4. Conclusion

We demonstrate a high-repetition-rate mJ IOPO laser with a QCW side-pumping diode stack. A theoretical model for generating $TEM_{n,0}$ mode in the diode-stack directly side-pumped resonator have been explored. We apply a hemispherical cavity for the Nd:YVO_4 laser and successfully generate $TEM_{0,0}$ mode and $TEM_{1,0}$ mode at 1064 nm by adjusting the displacement between the active medium and the laser axis. With the Cr^{4+}:YAG crystal, the output pulse energy reaches 3.05 mJ with the repetition rate up to 200 Hz. The experimental results for both free-running and PQS are confirmed to be consistent with the theoretical analysis. After inserting the KTP crystal with monolithic IOPO cavity for optimization, we observe the output pulse energy up to 1.2 mJ at 17.9-mJ threshold energy. We also confirm the spatial cleaning ability for the OPO resonator to generate an nearly $TEM_{0,0}$ mode.

Acknowledgments

The authors thank the National Science Council for the financial support of this research under Contract No. NSC100-2628-M-009-001-MY3.

#205652 - $15.00 USD Received 28 Jan 2014; revised 25 Feb 2014; accepted 26 Feb 2014; published 25 Mar 2014